Mapping Potential *Anopheles stephensi* Habitats for Implementing "Seek and Destroy" Malaria Larval Source Management in Kwale County, Kenya

Ariel Isabelle Burnett[1, *], Ricardo Izurieta[1], Ismael Hoare[1], Namit Choudhari[2], Jesse Casanova[3], Brooke Yost[1], Charles Mbogo[4], Joseph Mwangangi[5], Martin Rono[5], Anthony Masys[1], Benjamin George Jacob[1]

[1]College of Public Health, University of South Florida, Tampa, USA

[2]School of Geosciences, University of South Florida, Tampa, USA

[3]USF Health International, University of South Florida, Tampa, USA

[4]Kenya Medical Research Institute, Nairobi, Kenya

[5]Kenya Medical Research Institute, Kilifi, Kenya

Email address:

aiburnett@usf.edu (Ariel Isabelle Burnett)

[*]Corresponding author

Abstract: We will reveal specific locations of potential habitats of *Anopheles stephensi*, a new and invasive malaria vector, in Kwale, Kenya. Previous regression models have not been able to locate specific habitats of this malaria vector in Kenya. This publication seeks to determine locations of potential artificial water container habitats of *An. stephensi* via remote visual detection and determine geo-ecological factors that are associated with those habitats. The preliminary signature mapping of potential habitats was done by obtaining GPS coordinates of potential, capture point, sentinel site locations through visual remote sensing of artificial water containers using Google Earth. Using a second-order eigenfunction, eigendecomposition, spatial filter algorithm to determine clustering propensities or non-propensities of those mapped potential capture point, sentinel site larval habitats, we were able to eco-cartographically distinguish hot and cold spots on stratified, georeferenced, Land Use Land Cover (LULC) polygons, a Digital Elevation Model (DEM), and a Normalized Difference Vegetation Index (NDVI) map within ArcGIS Pro. The results showed that there was a strong tendency towards clustering (Moran's I=0.67, p<0.001) and potential habitat hotspots were more likely to occur in urban classified LULC, grid-stratified areas (51.28% and 46.15% of the hotspot locations were in urban commercial and urban residential land covers respectively). Moreover, the georeferenced hotspot locations of potential habitats were found at higher elevations than the coldspots (409.1± 6.112m vs 379.5 ± 21.51m) and the hotspot habitats were closely associated with soil and low vegetation (mean NDVI=0.121 ± 0.0661). When faced with this new vector, these ecological variables can be employed to spatially target and prioritize potential habitats for implementing "Seek and Destroy" larval source management programs.

Keywords: *Anopheles stephensi*, Artificial Containers, Eigendecomposition Kwale, Kenya

1. Introduction

The invasion of *Anopheles stephensi* in the Horn of Africa is an emerging threat that, if unchecked might constitute a risk for up to 126 million people in urban cities of Africa out of a total population of 1.2 billion [1]. This potent malaria vector [2] was first discovered on the African continent in Djibouti in 2012 and has since spread to Ethiopia, Sri Lanka and Sudan according to WHO Vector Alert 2019 and at the current expansion rate it is likely to become established across Africa

if nothing is done urgently to control and stop its spread [3]. Suspected to be transported by sea trade, as seen with other invasive mosquito species, coastal African countries closely connected to trade with *An. stephensi* endemic countries are considered at high risk for vector importation and the presence of this new vector has already been detected in Kenya, which frequently trades with India, Ethiopia, and Sudan [3, 4]. However, so far, the existence of *An. stephensi* has been detected accidentally, indicating the insufficient capacity of surveillance systems in the area to find or identify the vector [4]. More importantly, Africa's vector surveillance systems are lagging in monitoring changes in vector composition and distribution. Several initiatives to tackle the invasion are ongoing in the Horn of Africa, most of them focusing on vector surveillance and understanding the ecology of the vector. Nevertheless, there is a need to fund extensive training on vector surveillance system approaches to confirm its distribution near areas of high movement of humans, animals, and goods across international borders. *An. stephensi* has shown resistance to the insecticides recommended by WHO for insecticide treated nets and indoor residual spraying, hindering the control of this vector through these tools [5].

An. stephensi is a competent vector of *Plasmodium vivax* and *Plasmodium falciparum* and a probable vector of zoonotic malaria parasites [2]. Found to have both anthropophilic and zoophilic biting habits, the vector typically feeds during the twilight hours, contrary to the late night and early biting preferences of the dominant vector species in Kenya [1, 6]. Moreover, *An. stephensi* prefers to breed in clear and stagnant waters often found in artificial water containers [6-8]. In arid and semi-arid regions of Western India, malaria transmission was propagated due to the *An. stephensi* habitats within underground community "tanka" (earthen drinking water storage reservoir) and "beri" (step well) structures [9, 10]. Similarly, studies in Chennai, India reported that *An. stephensi* preferred to breed in man-made and artificial water containers, and 78.61% of the breeding habitats found were from overhead tanks [7, 8]. These improperly covered underground or overhead water tanks harbor mosquito larvae at high and consistent densities for year-round malaria transmission [8, 9].

Currently, little is known about the geospatial distribution of *An. stephensi* habitats in East Africa. Previously, Thomas [8] mapped out the distribution of *An. stephensi* breeding habitats in Chennai and analyzed their relationship to malaria cases within the city. However, this study focused more on the association of nearby breeding habitats with the intensity of malaria transmission [8], rather than the clustering tendencies of those habitats and ecological factors influencing them. In contrast, Sinka [1] has mapped the spread of *An. stephensi* habitats in cities across Asia and the Horn of Africa and utilized ecological factors associated with known *An. stephensi* habitats to create predictive models of other environmentally suitable areas at risk of importation of this new vector. Nevertheless, the study focused on more small-scale mapping of regions [1], instead of the large-scale mapping of precise locations in this study. Although mapping of *An. stephensi* habitats in Kenya have not yet been done,

Jacob [11] mapped the distribution of *An. gambiae* habitats in Kisumu and Malindi, Kenya. Utilizing remote sensing techniques, the study determined that ecological factors, such as changes in land use, could affect the distribution of anopheline larval habitats [11].

Therefore, the objectives of this publication will be to identify potential artificial water containers of *An. stephensi* via visual detection on Google Earth imagery. For our second objective, we spatially target and prioritize potential *An. stephensi* habitat estimators on classified land use land cover (LULC) using average slope coefficients and other catchment watershed variables from a Digital Elevation Model (DEM) and photosynthetic indices from a Normalized Difference Vegetation Index (NDVI). Finally, we will employ a second-order eigenfunction eigendecomposition algorithm to determine clustering propensities or non-propensities [i.e., hot/cold spots] of these mapped, potential, *An. stephensi* habitats to distinguish hot and coldspots on LULC, stratified polygons to predictively cartographically delineate geolocations in Kwale, Kenya, for "Seek and Destroy" larval source management programs. "Seek and Destroy" is a new real-time control measure for reducing larval, vector density in communities affected by malaria through habitat mapping for targeted treatment via geospatial artificial intelligence infused into an iOS application [12].

This research is to determine geolocations of aquatic habitats of *An. stephensi*, a major malaria mosquito vector that has recently arrived into East Africa from India. The purpose of this research is for mapping *An. stephensi* artificial water habitats to implement a larval source management program called "Seek and Destroy." The reason for implementing a larval control strategy specifically for *An. stephensi* is that there are already multiple malaria mosquito species throughout East Africa. Hence, controlling this vector is vital to stop the transmission of malaria. Currently, there are only three publications on the presence of *An. stephensi* in East Africa. Thus, the research question is: can we interpolate an *An. stephensi* habitat spectral signature to identify unknown locations of clustering and non-clustering artificial water containers that are suitable for *An. stephensi*.

2. Methodology

2.1. Study Site

Kwale County is the southernmost coastal county of Kenya, although most of the county is inland. It is located just south of Mombasa, a major Kenyan port city, and borders Tanzania to the north (Figure 1). It spans a land area of 8,267.1 km^2, though a majority of the 866,820 population lives within 90 km of the coastline, leading to a population density of 105 persons per km^2 [13, 14]. About 80% of the population's income comes from subsistence farming; however, only 30% of the population is considered food secure due to various conditions such as access to appropriate resources and climate change [15]. The county has a typical monsoon climate and two rainy seasons. The short rains begin in October and last

until December, after which it is hot and dry from January until April [16]. Then, the long rains typically start in March and continue until June or July, followed by cooler months [16]. The average temperature throughout the county ranges from 23° to 25°C, with higher temperatures usually along the coast [15].

Kwale (4°10'28" S latitude and 39°27'37" E longitude) is the capital of Kwale County, Kenya [17]. Located 30 km southwest of Mombasa and 15 km inland from the coast of the Indian Ocean, Kwale is a small town with an urban population of about 10,063 people [18]. The population is 48.6% male and 51.4% female [18]. Kwale has a large concentration of Digo and Duruma people, who are part of the Mijikenda ethnic group, and it is considered their main town [17].
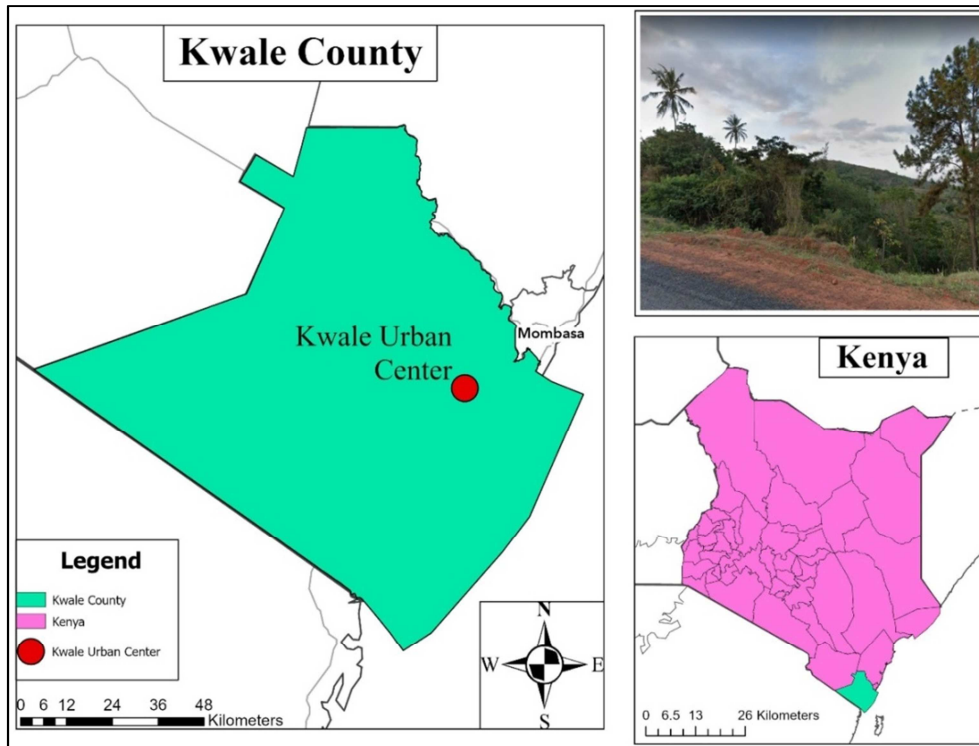

Figure 1. Study site map of Kwale, Kenya and an image depicting the typical terrain of the area.

2.2. Potential Habitats

Figure 2. Image of a water tank in urban Kwale.

Visual detection of potential habitats was done via Google Earth. The boundaries of the study area, urban Kwale center, were first delineated using the polygon tool, and it encompasses an area of about 7.5 km^2. After which, gridlines one-second latitude (~32 meters) and one second longitude (~32 m) apart were overlayed on the study area. Each cell created by the gridlines was methodically scanned for large artificial water reservoirs or artificial containers that could hold water, such as the typical water tank found in the area, as exemplified in Figure 2. 182 potential habitats were denoted with a placemark and labeled with a number and description indicating the type of habitat. The latitude, longitude, and elevation associated with each placemark were then transferred into an Excel spreadsheet for further analysis and mapping.

2.3. Spatial Autocorrelation Analyses

The assumption for spatial independence was tested for the remotely identified *An. stephensi* observations employing the Pearson product-moment correlation coefficient [i.e., Moran's Index (*I*)]. In statistics, Moran's *I* is a measure of spatial autocorrelation. Spatial autocorrelation is characterized by a correlation in a signal among nearby locations in space. Spatial autocorrelation is the correlation among values of a single variable strictly attributable to their relatively close locational positions on a two-dimensional surface, introducing a deviation from the independent

observation's assumption of the classical statistics [19].

Moran's *I* was employed as a diagnostic tool for quantitating model misspecifications, spatial non-homoscedasticity [i.e., uneven variance], and outliers in the satellite sensed, *An. stephensi* parameter estimators. Homoscedasticity describes a situation in which the error term (that is, the "noise" or random disturbance in the relationship between the independent variables and the dependent variable) is the same across all values of the independent variables [20]. The frequency dataset was stratified into georeferenced LULC classified groups of *An. stephensi* habitat proportions based on their occurrence abundance and distribution. Likewise, Moran's *I* was employed to determine if the dependent variables were clustered or randomly distributed within a geographic space in Kwale.

We employed R to generate Moran's *I* by computing the cross mean of Euclidean inter-site distances between stratified, *An. stephensi* habitat sampled, explanatory values that were geographic neighbors. Our first step in Moran's *I* analysis was to define "neighboring" polygons. [i.e., contiguous polygons, polygons within a certain Euclidean distance,] [21]. The LAGDISTANCE OPTION indicated the neighborhood size, which was important in the computation of the autocorrelation index for quantitating clustering propensities in the sampled variables. It is of note that lag distance in this research was dependent on the sampled county-level *An. stephensi* habitat parameter estimator sample dataset. Our goal was to create a variogram that invariably provided optimal estimates of spatial dependence for the underlying stochastic process within the dataset.

The compute statement allowed the averaging of binary spatial weights within the autocorrelation statistical process needed for the construction of Moran's *I* coefficient (an equivalent of regression slope for Moran's scatter plot). Using the values from LAGDISTANCE and MAXLAGS we constructed an *An. stephensi* habitat frequency model in R without the No variogram option to compute the empirical semivariogram. A variogram is often defined as a measure of spatial variability. [19] Our strategy was that by sampling stratified, *An. stephensi* habitat capture points close to each other, then this would produce typically similar outcomes compared to sampling for the capture points separated by larger distances in geographic space. Here the variogram distance measured the degree of dissimilarity γ(h) between the sampled, stratified, *An. stephensi* habitat data separated by a class of vectors h. If z(xi) and z(xj + h) were pairs of exploratory georeferenced breeding site aquatic foci samples lying within a given class of distance and direction, then N(h) was the number of data pairs within a land cover class. Subsequently, the experimental semivariogram was defined in R as the average squared difference between the components of the sampled, the *An. stephensi* habitat stratified data pairs in geographic space employing the following equation:

$$\gamma h = 12Nh \sum i = 1 \, Nhzx - xi + h2 \qquad (1)$$

This spatial variability measure is a semivariogram [21]. We

interpolated between the sample variogram and explanatory estimators. The variance of the entire dataset was re-defined as the sill and the distance at which the model semivariogram met the data set variance we defined as the range.

We specified the CL option in the COMPUTE statement to calculate the 95% confidence limits for the classical semivariance. The Compute Statement described how to use the ALPHA= option to specify a different confidence level in the *An. stephensi* habitat frequency, forecast, vulnerability, county-level, artificial water container model. We requested a robust version of the semivariance with the ROBUST option in the COMPUTE statement. R rendered a plot showing both the classical and the robust empirical semivariograms. The Plot option to specify different instances of plots was featured in the empirical semivariogram. In addition, the autocorrelation Moran's *I* statistics under the assumption of randomization using binary weights was generated. The output from the requested autocorrelation predictive, probabilistic, spatiotemporal analysis included the observed, computed Geary's *C* coefficients. The finely tabulated expected value and standard deviation for each sampled stratified, explanatory covariate, the corresponding Z score, and the p-value were calculated in the Pr >j Z j column. The low p-values suggested non-zero autocorrelation for both statistics types. Note that a two-sided p-value was generated, which was based on the probability that the observed, *An. stephensi* habitat frequency coefficients lay farther away from j Z j on either side of the coefficient's expected value—that is, lower than Z or higher than Z. The sign of Z for both Moran's *I* and Geary's *C* coefficients can indicate a latent positive or negative autocorrelation [19]. The output randomization estimates from the stratified autocorrelation frequency model were then evaluated in a spatial error (SE) model. An autoregressive model was employed whereby a geosampled, temporally dependent, socioeconomic stratified variable, Y, as a function of nearby sampled *An. stephensi* habitat frequency Y values [i.e., an autoregressive response (AR) or spatial linear (SL) specification] and/or the residuals of Y as a function of nearby Y residuals [i.e., an AR or SE specification]. Distance between frequency-sampled, stratified *An. stephensi* habitat predictors were subsequently defined in terms of an *n*-by-*n* geographic weights matrix, C, whose c_{ij} values were 1 if the sampled *i* and *j* were deemed nearby and 0 otherwise. Adjusting this matrix by dividing each row entry by its row sum, with the row sums given by C1, converted this matrix-to-matrix W.

All residual estimates from the model were then evaluated in a SE model. An autoregressive model was employed that used a sampled habitat variable, Y, as a function of nearby sampled habitat Y values [i.e., an autoregressive response (AR) or spatial linear (SL) specification] and/or the residuals of Y as a function of nearby Y residuals [i.e., an AR or SE specification]. Distance between sampled *An. stephensi* habitat geolocations was definable in terms of an *n*-by-*n* geographic weights matrix, C, whose c_{ij} values were 1 if the sampled An. *stephensi* habitat locations *i* and *j* were deemed nearby, and 0 otherwise. Adjusting this matrix by dividing

each row entry by its row sum, with the row sums given by C1, converted this matrix to matrix W [19].

2.4. Mapping Ecological Models

After spatial autocorrelation analysis, potential *An. stephensi* habitat hotspots with 95% confidence intervals and coldspots with 95% confidence intervals were obtained from the data set using ArcGIS Pro. Two separate layers were then generated: one for potential habitat locations within significant hotspots and one for potential habitat locations within significant coldspots. Three separate models were also created to compare the geo-ecological variables associated with potential *An.*

stephensi habitats: Land Use Land Cover (LULC), Digital Elevation Model (DEM), and Normalized Difference Vegetation Index (NDVI). For the first model, the satellite imagery of the study area was utilized to manually create a LULC map. Using the criteria outlined in Table 1, color-coded polygons created with Google Earth and Google Earth Pro tools, were overlayed on the satellite imagery to divide the study area into urban commercial, urban residential, rural farmland, and forestland land covers (Figures 3, 4). The hotspot and coldspot locations were then overlayed on the LULC model and the percentage of hotspot and coldspot locations found within each type of landcover was determined.
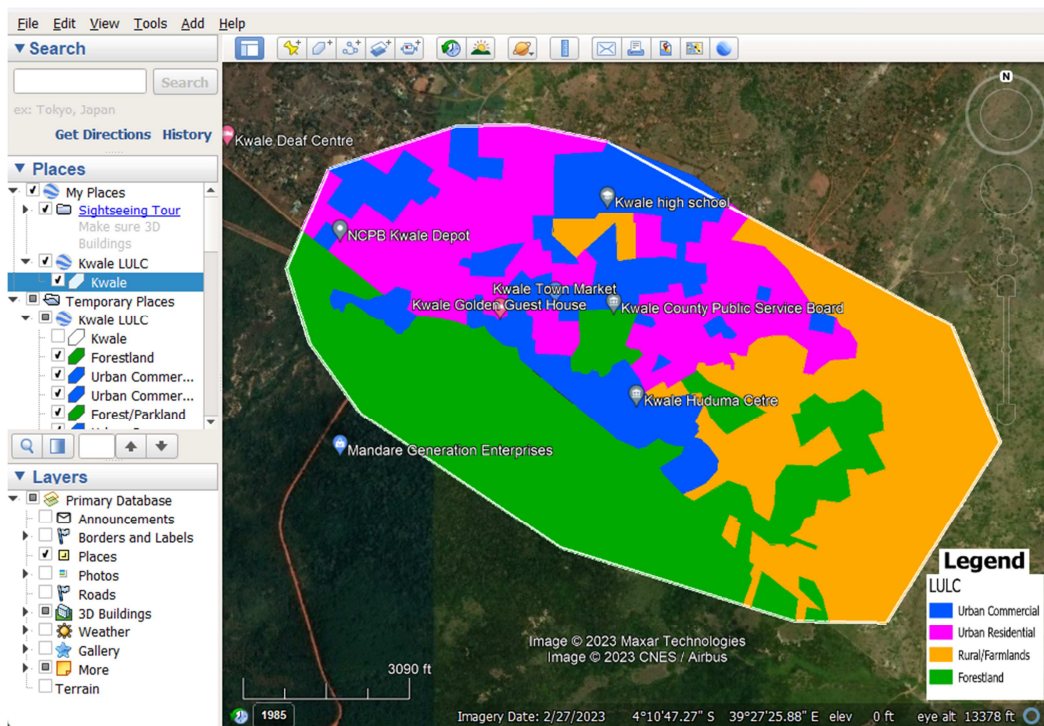

Figure 3. *Creation of LULC map of Kwale urban center using Google Earth Pro.*

Figure 4. *Close up of LULC map in Google Earth and the differing landcovers.*

Table 1. *Descriptions and criteria of LULC classifications.*

Land Use Land Cover Type	Description
Urban Commercial	Structured layout of buildings near large parking lots; large paved or dirt roads; low vegetation; and businesses, schools, or government offices labelled on the satellite image.
Urban Residential	Moderately condensed buildings in a disorderly layout, smaller paved or dirt roads, light vegetation, and unlabelled buildings.
Rural Farmland	Cultivated lands, medium to light vegetation, dirt roads, sporadic man-made structures, and sparsely populated.
Forestland	Dense vegetation and little to no man-made structures.

The DEM and NDVI maps of the study area were made within ArcGIS Pro after gathering satellite data from the Sentinel-2 satellite. The DEM satellite data was taken on June 27, 2007 (12.5 m resolution) and the NDVI satellite image was retrieved on March 1, 2023. After overlaying the hotspot and coldspot locations on each model, we extracted the elevations and NDVI score associated with each point on the map. Then, the average elevation and NDVI scores for hotspot locations and coldspot locations were calculated.

3. Results

The n-by-1 vector $x = [x_1 \cdots x_n]^T$ contained measurements of a quantitative variable for n spatial units and n-by-n spatial weighting matrix W. The formulation for the Moran's index of spatial autocorrelation used in this research was:

$$I(x) = \frac{n\sum_{(2)}w_{ij}(x_i-\bar{x})(x_j-\bar{x})}{\sum_{(2)}w_{ij}\sum_{i=1}^{n}(x_i-\bar{x})^2} \qquad (2)$$

where $\sum_{(2)}\sum_{i=1}^{n}\sum_{j=1}^{n}$ with i ≠ j

The values w_{ij} were spatial weights stored in the symmetrical matrix W [i.e., $(w_{ij} = w_{ji})$] that had a null diagonal $(w_{ii} = 0)$. In this research the matrix was initially generalized to an asymmetrical matrix W. Matrix W can be generalized by a non-symmetric matrix W^* by using $W = (W^* + W^{*T})/2$ [18]. Moran's I was rewritten using matrix notation:

$$I(x) = \frac{n}{(1^tW1)}\frac{x^tHHWHHx}{x^THHx} = \frac{n}{1^TW1}\frac{x^{THWHx}}{x^THx} \qquad (3)$$

where H = $(I - 11^T/n)$ was an orthogonal projector verifying that $H = H^2$, (i.e., H was independent). Features of matrix W for analyzing of An. *stephensi* habitat data include that it: is a stochastic matrix, expresses each observed value y_i as a function of the average of location I's nearby data, and allows a single spatial autoregressive parameter, ρ, to have a maximum value of 1.

The final model reveals a strong tendency for positive spatial autocorrelation in the *An. stephensi* habitat data (Moran's $I = 0.67$, p<0.001) (Figure 5). Of the 182 potential *An. stephensi* habitats found, 120 potential habitats were determined to be significantly associated with either a hotspot or coldspot. Seventy-eight locations were within a hotpot with 95% confidence, and forty-two locations were within a coldspot with 95% confidence. Based on the LULC map, the potential habitat hotspot locations were mainly found in urban commercial (51.58%, N = 40) and urban residential areas (46.15%, N = 36) (Table 2). Only 2.56% (N = 2) of the hotspot locations were within rural/farmland areas and no hotspot potential habitats were located within the forestlands (Figure 6). In comparison, most of the potential habitat coldspot locations were also found within urban land covers, but there was a higher percentage of coldspot habitats located within urban residential (47.62%, N = 20) as compared to urban commercial (28.57%, N = 12). Moreover, in contrast to the hotspot coverage of potential habitats, there were significantly more potential habitats within the coldspot that were located within rural farmland land cover (19.05%, N = 8) and 4.762% (N = 2) of the coldspot habitats were located within the forestlands.
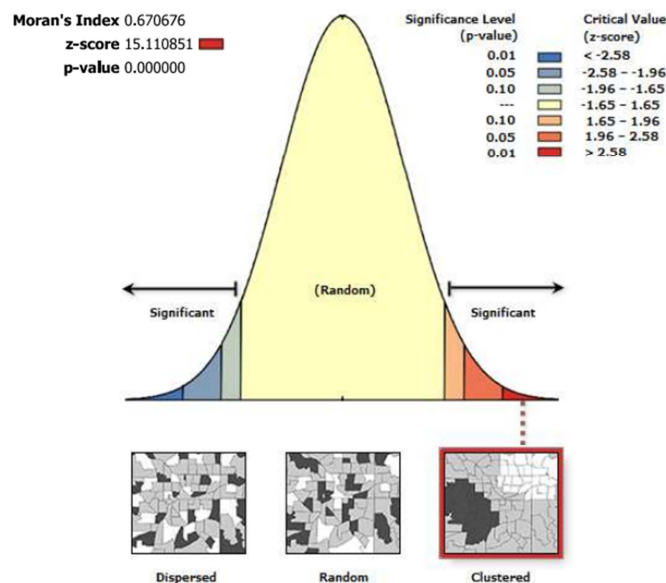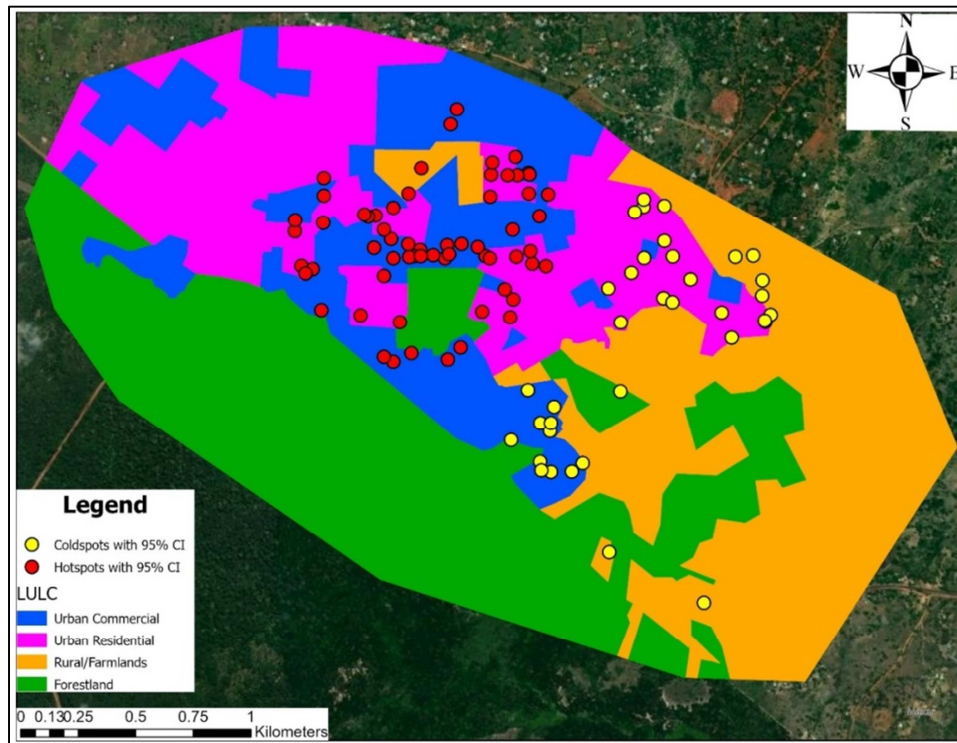

Figure 5. *Results of the autocorrelation analysis.*

***Table 2.** LULC distribution of potential An. stephensi habitats within hotspots and coldspots.*

Land Use Land Cover	Hotspot		Coldspot	
	Number (N=78)	Percentage (%)	Number (N=42)	Percentage (%)
Urban Commercial	40	51.28%	12	28.57%
Urban Residential	36	46.15%	20	47.62%
Rural Farmland	2	2.564%	8	19.05%
Forestland	0	0%	2	4.762%

***Figure 6.** Significant clusters of potential An. stephensi habitats overlayed on an LULC map of the urban Kwale center.*
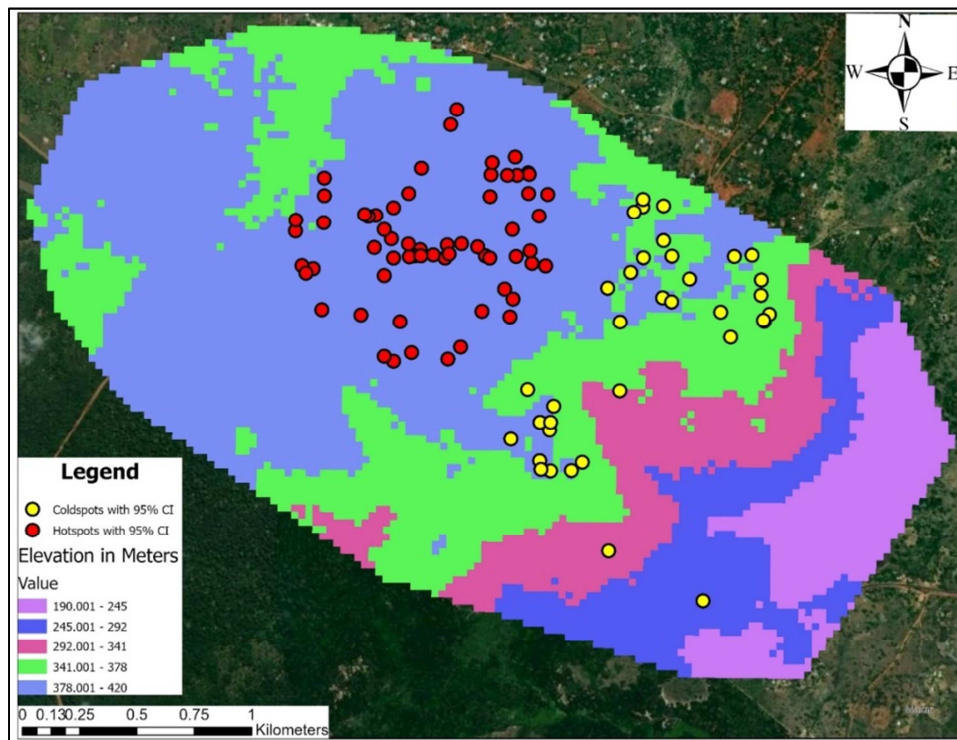
***Figure 7.** Significant clusters of potential An. stephensi habitats overlayed on a DEM map of the urban Kwale center.*
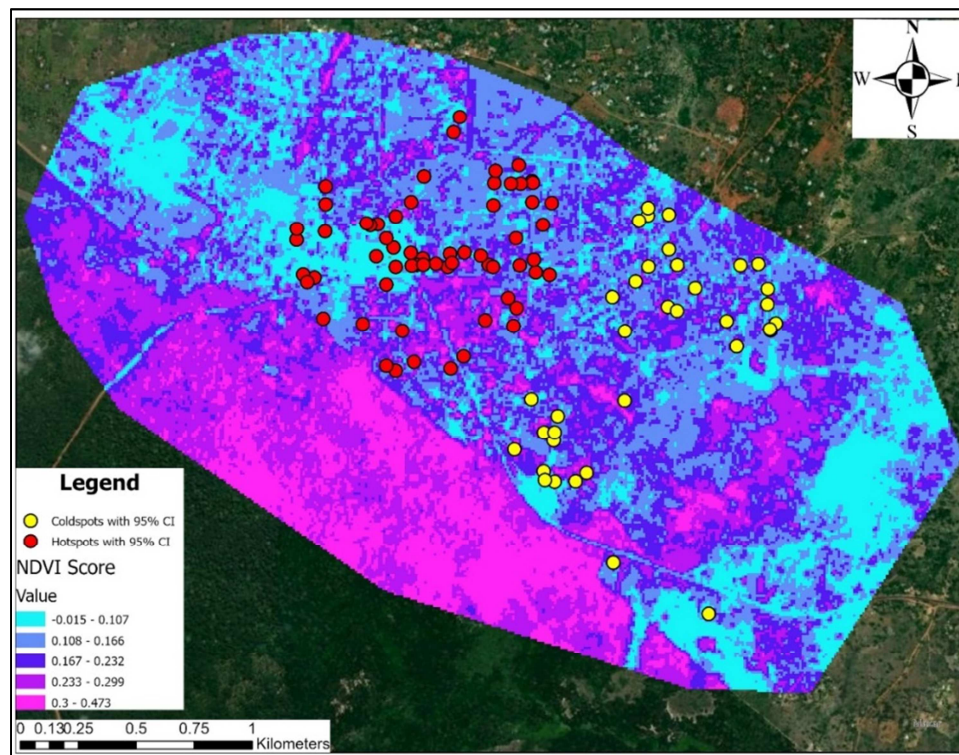
Figure 8. *Significant clusters of potential An. stephensi habitats overlayed on a NDVI map of urban Kwale center.*

The results from the DEM model revealed a slight difference in elevations for the potential habitats within the hotspot and within the coldspot. The mean elevation associated with the potential *An. stephensi* habitats located within hotspots was 409.1 ± 6.2 m. In contrast, the potential habitats within the coldspot were, on average, at a slightly lower elevation of 379.5 ± 21.5 m. Moreover, as seen by the DEM model, potential habitats clustered in an area of higher elevation that was surrounded by slightly lower elevation (Figure 7). The NDVI model also revealed slight differences in the mean NDVI scores of the potential habitats within hotspots and coldspots. The potential habitats within the hotspot had an NDVI score of 0.121 ± 0.066, and the potential habitats within the coldspot had a slightly higher NDVI score of 0.168 ± 0.051 (Figure 8). However, considering the potential error, no significant difference was found between the NDVI scores of the potential *An. stephensi* habitats that were found within the hotspot versus the coldspot. Similarly, the mean NDVI scores for the hotspot and coldspot potential habitats were both associated with low vegetation.

4. Discussion

Potential *An. stephensi* artificial water container habitat hot and cold spots occur in urban commercial and urban residential landcover. The strong clustering of potential *An. stephensi* habitats in urban areas is likely to contribute to the mosquito's presence as a vector of concern, and the vector's ability to thrive within urban environments [1, 6]. The most probable reason for this is because larger anthropogenic populations would have more artificial water containers. The

potential habitats, such as artificial water tanks and tires, are connected to human activity; thus, it would be logical that they would be clustered in densely populated areas. Moreover, studies on the recent expansion of this vector into new territories confirm the likelihood of *An. stephensi* habitation within urban commercial and residential areas. A study detailing the 2017 emergence of this new vector in Sri Lanka determined that *An. stephensi* larvae were found in sites with urban or semi-urban characteristics [22]. Similarly, a 2020 study of the spread of this new vector in Ethiopia also highlighted that *An. stephensi* was first detected in urban areas [23]. The concentration of viable habitats and the proximity to large anthropogenic populations, previously unexposed to malaria, in these settings exacerbates the potentiality of urban malaria epidemics, and it is imperative that surveillance and larval source management systems, such as "Seek and Destroy" focus their efforts in these areas. Further, sustaining "Seek and Destroy" seasonally would allow finer spatial targeting of artificial water containers in urban residential and commercial properties using drone/satellite remote sensing data.

"Seek and Destroy" is a program that was created by Dr. Benjamin Jacob with the aim of working toward the elimination of malaria in affected communities. At its inception, "Seek and Destroy" has two functions: the first is at the implementation level, and the second is at the policy level. At the implementation level, "Seek and Destroy" uses new technology coupled with proven methodologies used in larval source management techniques. New technologies used include unmanned aerial vehicles, artificial intelligence, machine learning algorithms, GIS, and iOS-integrated

dashboards, among other technologies, to decrease the time lag in real-time data that can be used for evidence-based decision-making. The aim of "Seek and Destroy" is to focus on habitats where *Anophelines* oviposit to eliminate the vector where it is concentrated, immobile, and accessible. The techniques used are the basis of larval source management, which includes activities such as burying habitats, habitat modification, and targeted and responsible larviciding. At the policy level, "Seek and Destroy" brings together stakeholders from the political sector, the NGO sector, and university researchers in a way that will allow for decision-making to take place with real-time data and to create health systems strengthening policy to scale up this program from a test site to an entire country.

Within an urban setting, potential *An. stephensi* habitats also tend to cluster in areas of slightly higher elevation. This study found that potential habitats within a hotspot were all condensed in the area of Kwale with the highest elevations. All the potential hotspot locations were found in an elevation range of about 390-420 m, which is within the previously found viable elevations for the vector [24]. Pemola Devi and Jauhari [24] determined that *An. stephensi* mosquitos in the Garhwal region of India are found within tropical (300-1000 m) elevations, and apart from one potential coldspot habitat found at around 270 m elevation, our potential *An. stephensi* habitats fall within the known range. Moreover, the potential habitats tend to cluster in an elevated area of Kwale, which is surrounded by slightly lower elevations. This typographical result coincides with a study performed in Chennai, which found that malaria infections attributed to *An. stephensi* clustered in areas with higher elevations that were surrounded by slightly lower elevations [7]. However, they surmised that these results are due to mosquitoes breeding in the surrounding lower-lying areas before emerging and traveling to higher elevations for bloodmeals. Our results show that potential habitats also cluster in these topographical areas; thus, there is a possibility that the high rates of malaria could be due to the proximity of numerous *Anopheline* habitats instead.

Clusters of potential *An. stephensi* habitats in Kwale, Kenya are closely associated with areas of low vegetation. Our results coincide with Pemola Devi and Jauhari's [24] characterization of *An. stephensi* breeding habitats in the western Himalayas, which are typically found in areas of thin or negligible vegetation. Similarly, Sinka [6] concluded that although *An. stephensi* habitats can be seen in areas with higher concentrations of plants and algae, the typical larval site characteristic of their habitats is an area with no vegetation. While there were no significant differences in the mean NDVI scores of potential hotspot and coldspot habitats in our study, both sets of habitats had low mean NDVI scores, which are indicative of low vegetation. These results could be caused by the high number of potential habitats that were found within urban areas, which typically have low vegetation. In fact, the majority of the potential coldspot habitats were within urban commercial and residential land covers. Moreover, when searching for potential habitats,

certain visibility is required from satellite imagery (< 20 percent cloud cover). Therefore, potential habitats in areas with low vegetation cover have higher visibility and are more likely to be detected remotely. Nevertheless, artificial water containers are associated with human activity, and areas with human activity are likely to have lower NDVI scores. Understanding the distribution of potential habitats in close proximity to anthropogenic activity and populated areas can provide better information for prevention programs, as vectors that emerge from these habitats are more likely to inoculate human hosts.

Artificial water containers in slightly elevated urban areas with low vegetation are ideal candidates for potential *An. stephensi* habitats. Utilizing the ecological and typographical results from our study we can construct robust surveillance systems for the timely detection of this emerging vector in communities deemed at-risk for invasion. Moreover, the clustering propensities of potential *An. stephensi* habitats can inform "Seek and Destroy" larval management systems and affected communities can efficiently use limited resources by prioritizing clusters of potential habitats for treatment.

There are some limitations in the results, however, as there is a possibility of bias. Since the detection of habitats was performed through manual remote visual detection, there is a possibility for human error when searching for and labeling artificial containers. Nevertheless, potential bias was minimized by the use of gridlines, and each gridded area was scanned with the same amount of effort; therefore, any possible errors or missed habitats were evenly distributed throughout the study area. Errors may have also arisen due to the visibility of potential habitats, which could have been compromised by vegetation or other structures, as mentioned previously. Likewise, Google Earth images of the study area consist of bands of satellite images taken at different times and with varying quality, which could have further obscured the detection of artificial water containers. Similarly, our manual method of creating the LULC map may lead to some limitations due to the difficulty in classifying between urban-rural and urban commercial areas. In contrast to areas with urban planning, homesteads and businesses are often intermingled in Kwale, complicating the distinctions between the two. Moreover, many of the classifications rely on the Google Earth identification of businesses, schools, and government buildings. Therefore, if commercial businesses were not up to date or properly labeled, then that could lead to improper classification. Nevertheless, the distinction between urban areas and rural farms or forestlands was clear and the clustering propensities of potential habitats in urban areas in Kwale is undisputable.

Further studies are suggested to confirm our results through field verification of artificial water container habitats in Kwale. Similarly, studies on the detection and counts of *An. stephensi* larvae within these habitats could bolster studies on the clustering propensities of these habitats and factors that may influence these clustering behaviors. Moreover, "Seek and Destroy" larval management strategies should be implemented for spatially targeting *An. stephensi* larvae in

urban ecosystems. Therefore, further studies on the effectiveness and efficiency of this larval management system compared to the employment of larvicide can influence the direction of future urban mosquito management programs.

5. Conclusion

Integration of remote visual detection via satellite data and GIS algorithms can transform monitoring and surveillance methods in Kwale, Kenya. Using Google Earth and ArcGIS software, the study determined that types of land covers, elevations, and vegetation index influence the spatial dynamics of potential *An. stephensi* habitats. These factors can then be utilized to optimize monitoring methods and prioritize larval management systems in place. Typical malaria and vector surveys in Kenya consist of ground teams walking and covering entire communities in search of habitats. However, this is time-consuming and expensive as large teams must be paid for each day of monitoring. In contrast, we can implement overhead capabilities, such as satellite data, to geospatially target clusters of potential habitats and optimize vector surveys. Moreover, we can supplement malaria prevention tools currently in place with new methods of larval management that employ the same satellite data and ArcGIS algorithms. As we move towards eradication of malaria, we can utilize these technologies to prioritize clusters of artificial water containers for efficient vector control programs by determining and mapping areas for the purposes of "Seek and Destroy" larval management.

References

[1] Sinka, M. E., et al., A new malaria vector in Africa: Predicting the expansion range of *Anopheles stephensi* and identifying the urban populations at risk. *Proc Natl Acad Sci U S A,* 2020. 117 (40): p. 24900-24908.

[2] Tadesse, F. G., et al., *Anopheles stephensi* Mosquitoes as Vectors of *Plasmodium vivax and falciparum*, Horn of Africa, 2019. *Emerg Infect Dis,* 2021. 27 (2): p. 603-607.

[3] Ahn, J., et al., Modeling marine cargo traffic to identify countries in Africa with greatest risk of invasion by Anopheles stephensi. Sci Rep, 2023. 13 (1): p. 876.

[4] Ndenga, B. A., et al., Serendipitous detection of Anopheles stephensi in Kisumu, Kenya in June 2022. medRxiv, 2023: p. 2023.05.02.23289394.

[5] Yared, S., et al., Insecticide resistance in Anopheles stephensi in Somali Region, eastern Ethiopia. Malar J, 2020. 19 (1): p. 180.

[6] Sinka, M. E., et al., The dominant Anopheles vectors of human malaria in the Asia-Pacific region: occurrence data, distribution maps and bionomic précis. Parasit Vectors, 2011. 4: p. 89.

[7] Kumar, D. S., et al., Spatial trend, environmental and socioeconomic factors associated with malaria prevalence in Chennai. Malar J, 2014. 13: p. 14.

[8] Thomas, S., et al., Overhead tank is the potential breeding habitat of Anopheles stephensi in an urban transmission setting of Chennai, India. Malar J, 2016. 15 (1): p. 274.

[9] Singh, H., et al., The impact of mosquito proof lids of underground tanks "tanka" on the breeding of Anopheles stephensi in a village in western Rajasthan, India. Malar J, 2021. 20 (1): p. 412.

[10] Tyagi, B. K. and S. P. Yadav, Malariological and sociological significance of 'tanka' and 'beri' in the Thar Desert, Western Rajasthan, India. Journal of Arid Environments, 1996. 33 (4): p. 497-501.

[11] Jacob, B. G., et al., Environmental abundance of Anopheles (Diptera: Culicidae) larval habitats on land cover change sites in Karima Village, Mwea Rice Scheme, Kenya. Am J Trop Med Hyg, 2007. 76 (1): p. 73-80.

[12] Jacob, B. G., et al., Geospatial artificial intelligence infused into a smartphone drone application for implementing 'Seek and Destroy' in Uganda. American Journal of Entomology, 2021. 5 (4): p. 92-109.

[13] Kenya National Bureau of Statistics, The 2019 Kenya Population and Housing Census Volume I: Population by County and Sub-County, Kenya National Bureau of Statistics, Editor. 2019: Nairobi, Kenya.

[14] Snow, R. W., et al., Changing Malaria Prevalence on the Kenyan Coast since 1974: Climate, Drugs and Vector Control. PLoS One, 2015. 10 (6): p. e0128792.

[15] The Ministry of Agriculture, Livestock and Fisheries (MoALF), Climate Risk Profile for Kwale County. Kenya County Climate Risk Profile Series, MoALF, Editor. 2016: Nairobi, Kenya.

[16] Wikimedia Foundation, Kwale County. June 23, 2023; Available from: https://en.wikipedia.org/wiki/Kwale_County.

[17] Wikimedia Foundation, Kwale. April 1, 2023; Available from: https://en.wikipedia.org/wiki/Kwale.

[18] Kenya National Bureau of Statistics, 2019 Kenya Population and Housing Census Volume II: Distribution of Population by Administrative Units, Kenya National Bureau of Statistics, Editor. 2019.

[19] Griffith, D., Spatial Autocorrelation and Spatial Filtering: Gaining Understanding through Theory and Scientific Visualization. 2003.

[20] Hosmer, D. W. and S. Lemeshow, Applied Logistic Regression. 2000.

[21] Cressie, N. A. C., Statistics for Spatial Data. 1993, John WIley & Sons, Inc.

[22] Surendran, S. N., et al., Anthropogenic Factors Driving Recent Range Expansion of the Malaria Vector Anopheles stephensi. Front Public Health, 2019. 7: p. 53.

[23] Balkew, M., et al., Geographical distribution of Anopheles stephensi in eastern Ethiopia. Parasit Vectors, 2020. 13 (1): p. 35.

[24] Pemola Devi, N. and R. K. Jauhari, Mosquito species associated within some Western Himalayas phytogeographic zones in the Garhwal region of India. J Insect Sci, 2007. 7: p. 1-10.